

ANDREAS RIEDER

Embedding and a priori wavelet-adaptivity for Dirichlet problems

ESAIM: Modélisation mathématique et analyse numérique, tome 34, n° 6 (2000),
p. 1189-1202

http://www.numdam.org/item?id=M2AN_2000__34_6_1189_0

© SMAI, EDP Sciences, 2000, tous droits réservés.

L'accès aux archives de la revue « ESAIM: Modélisation mathématique et analyse numérique » (<http://www.esaim-m2an.org/>) implique l'accord avec les conditions générales d'utilisation (<http://www.numdam.org/conditions>). Toute utilisation commerciale ou impression systématique est constitutive d'une infraction pénale. Toute copie ou impression de ce fichier doit contenir la présente mention de copyright.

NUMDAM

Article numérisé dans le cadre du programme
Numérisation de documents anciens mathématiques
<http://www.numdam.org/>

EMBEDDING AND *A PRIORI* WAVELET-ADAPTIVITY FOR DIRICHLET PROBLEMS

ANDREAS RIEDER¹

Abstract. The accuracy of the domain embedding method from [A. Rieder, *Modél. Math. Anal. Numér.* **32** (1998) 405–431] for the solution of Dirichlet problems suffers under a coarse boundary approximation. To overcome this drawback the method is furnished with an *a priori* (static) strategy for an adaptive approximation space refinement near the boundary. This is done by selecting suitable wavelet subspaces. Error estimates and numerical experiments validate the proposed adaptive scheme. In contrast to similar, but rather theoretical, concepts already described in the literature our approach combines a high generality with an easy-to-implement algorithm.

Mathematics Subject Classification. 65N30, 65N50.

Received: March 9, 2000. Revised: July 31, 2000.

1. INTRODUCTION

In [33] we proposed and analyzed a domain embedding method for the numerical solution of the Dirichlet boundary value problem (1.1) of second order:

$$-\operatorname{div}(A \nabla u) + \alpha u = f \quad \text{in } \Omega \subset \mathbb{R}^d, \quad (1.1a)$$

$$u = g \quad \text{on } \partial\Omega. \quad (1.1b)$$

It was shown that the resulting algorithm:

- (i) allows Cartesian grids resulting in simple data structures and fast memory access times;
- (ii) requires only little geometric information, namely, a digitalized version of the indicator function of Ω .

Unfortunately, there is a price to pay. As uniform Cartesian grids cannot be aligned accurately enough with the boundary of Ω the accuracy of the obtained numerical solution deteriorates near $\partial\Omega$. Consequently, optimal error estimates are only available in the interior of Ω . In the present paper we introduce an approach to cure this dilemma by refining the Cartesian mesh near $\partial\Omega$. The tool we rely on is a wavelet splitting of the underlying approximation space.

Systems of elliptic equations closely related to (1.1) naturally arise in simulating incompressible viscous flow by operator splitting techniques, see *e.g.* [22]. Such operator splitting techniques are particularly efficient when combined with domain embedding (see *e.g.* [23–25]).

Keywords and phrases. Boundary value problem, fictitious domain, Galerkin scheme, biorthogonal wavelet system, adapted grid.

¹ Institut für Wissenschaftliches Rechnen und Mathematische Modellbildung (IWRMM), Universität Karlsruhe, 76128 Karlsruhe, Germany. email: andreas.rieder@math.uni-karlsruhe.de

The paper is outlined as follows. In the next section we briefly recall our fictitious domain (or embedding) approach from [33]. The first part of Section 3 collects briefly some facts from wavelet theory which we will need for our investigations. We are then ready for the Galerkin discretization of the fictitious domain version of (1.1) using scaling function spaces (Sect. 3.2). Looking at error estimates we motivate the need of a finer discretization near the boundary of Ω . The technical details of our static adaptive scheme are presented in Section 4. Roughly speaking, we sparse the approximation space by removing unnecessary wavelets. A rigorous error analysis justifies our adaptive strategy. We illustrate our theoretical estimates by computational experiments in Section 5. The paper ends with some concluding remarks.

We freely admit that our obvious technique for the boundary refinement was already considered before in connection with wavelets and shift-invariant spaces by Jaffard [27] and Oswald [31]. However, Jaffard's investigation was limited to a very delicate wavelet-system (see [28]), which is hard to use in numerical computations (indeed, Jaffard only presented some numerical 1D-experiments and the author is not aware of an implementation in higher dimensions). Nevertheless, we use the very same principle here.

From a geometric point of view our and Oswald's [31] approaches are even more related: we both discretize the underlying domain by cubes getting smaller towards the boundary (the Jaffard-Meyer wavelets are adapted to the boundary). In a very general framework Oswald studied to which extent shift invariant spaces may be used to obtain accurate solutions to elliptic problems. This means: we cannot obtain error estimates which are asymptotically better than Oswald's. The accuracy of our scheme is the best possible which, unfortunately, leads to an efficient algorithm (in terms of accuracy related to the number of unknowns) only for $d = 2$ and second-order wavelet systems. The numerical scheme we propose and analyze here may be viewed as a realization of the more abstract concepts of Jaffard and Oswald.

Finally we like to mention other approaches to carry over the wavelet machinery from rectangular domains to arbitrary shaped bounded domains. We only refer to [5, 15]. These techniques are based on domain decomposition and/or parametric mappings. They share the drawback of having to be adapted very carefully to the geometry of the underlying domain. On the other side they guarantee optimal convergence rates with an optimal number of unknowns. In [16] Dahmen and Stevenson construct local wavelet bases for C^0 Lagrange finite element spaces, thus enabling wavelet techniques in the finite element context.

The potential of wavelets for the adaptive discretization of partial differential equations has been employed before in different settings (see *e.g.* [4, 9, 19, 20], and Chap. II of [13]). In these papers *a posteriori* wavelet-adaptivity is investigated where error indicators steer a local refinement of the approximation spaces. Very recently, Cohen *et al.* [7] proposed such an adaptive wavelet algorithm for elliptic operators which converges with optimal order (in a Besov scale) and which has optimal computational complexity. Numerical experiments have been reported by Barinka *et al.* [1].

2. FICTITIOUS DOMAIN FORMULATION

We quickly recall our fictitious domain formulation of the Dirichlet problem (1.1). For more details and references see [33].

Beforehand we specify our requirements. Let $\Omega \subset \mathbb{R}^d$, $d \geq 2$, be a bounded domain with finite perimeter and Lipschitz continuous boundary. The coefficient matrix $A : \Omega \rightarrow \mathbb{R}^{d \times d}$ is required to have smooth entries and to be uniformly positive definite on Ω . Let α be smooth and non-negative.

We further assume that $f \in L^2(\Omega)$ and $g \in H^{1/2}(\partial\Omega)$. For a definition of the L^2 -Sobolev spaces $H^s(\Omega)$ and $H^s(\partial\Omega)$ we refer, *e.g.*, to [35].

Under these hypotheses the boundary value problem (1.1) admits a unique weak solution $u \in H^1(\Omega)$, see *e.g.* [21, 26].

The point of departure is the same for all fictitious domain techniques. We embed $\bar{\Omega}$ in a larger rectangular domain \square whose edges are aligned with the coordinate axes in \mathbb{R}^d . Next we extend the differential equation (1.1) to a boundary value problem over \square . In formulating the extended boundary value problem we have the freedom to impose boundary conditions on $\partial\square$ making Galerkin type discretizations as convenient as possible. We will work with periodic boundary conditions allowing a lucid presentation of our ideas (but the methodology can be

carried over to Dirichlet boundary as well as Neumann boundary constraints). Further, we restrict ourselves to the unit box $\square = (0, 1)^d$ as fictitious domain. This means no loss of generality.

Identifying 1-periodic functions ($v(\cdot + k) = v(\cdot)$ for all $k \in \mathbb{Z}^d$) with functions defined on the torus \mathcal{T}^d (and vice versa) we consider $H^r(\mathcal{T}^d)$, the r th order Sobolev space on the manifold \mathcal{T}^d , as a Sobolev space of periodic functions.

Let $\tilde{A} : \square \rightarrow \mathbb{R}^{d \times d}$ and $\tilde{\alpha} : \square \rightarrow \mathbb{R}$ be extensions of A and α , respectively, that is, $\tilde{A}|_{\Omega} = A$ and $\tilde{\alpha}|_{\Omega} = \alpha$. With those we define the bilinear form a by

$$a(w, v) := \int_{\square} ((\tilde{A}\nabla w) \cdot \nabla v + \tilde{\alpha} w v) \, dx.$$

Let $\gamma : H^1(\Omega) \rightarrow H^{1/2}(\partial\Omega)$ be the trace operator. We define the variational problem,

$$\begin{cases} \text{find } \tilde{u} \in H^1(\mathcal{T}^d) \text{ with } \gamma\tilde{u} = g \text{ such that} \\ a(\tilde{u}, v) = \langle \tilde{f}, v \rangle_{L^2(\mathcal{T}^d)} \quad \forall v \in H^1(\mathcal{T}^d) \text{ with } \gamma v = 0, \end{cases} \tag{2.1}$$

which is our fictitious domain formulation of the Dirichlet problem (1.1). Here, $\tilde{f} : \square \rightarrow \mathbb{R}$ is an L^2 -extension of f .

Remark 2.1. (a) Of course, the fictitious domain formulation (2.1) depends crucially on the existence of the extensions \tilde{A} , $\tilde{\alpha}$, and \tilde{f} . In many applications, however, A , α , and f are explicitly known as restrictions of functions defined on \mathbb{R}^d . Then the needed extensions come for free.

(b) For a fictitious domain formulation of (1.1a) furnished with a Neumann boundary constraint we refer to [32].

The following lemma relates the fictitious domain formulation (2.1) to the boundary value problem (1.1). For a proof see Chapter 2 in [33].

Lemma 2.2. *Let the extensions \tilde{A} , $\tilde{\alpha}$ satisfy the same restrictions over \square as A and α over Ω . Then, (2.1) has a unique solution $\tilde{u} \in H^1(\mathcal{T}^d)$ coinciding with the weak solution u of (1.1) on Ω .*

In the sequel we will not distinguish anymore between quantities defined on Ω and their extensions to \square , that is, $u = \tilde{u}$, $A = \tilde{A}$, $\alpha = \tilde{\alpha}$, and $f = \tilde{f}$.

3. GALERKIN DISCRETIZATION

This section is devoted to the non-conforming Galerkin discretization of the variational problem (2.1) introduced in [33]. The required approximation spaces will be generated by translated and dilated versions of a single scaling function. Following we collect some facts on scaling functions which will be important throughout the paper.

3.1. Scaling function spaces

A function $\varphi \in L^2(\mathbb{R})$ is called *scaling function* if it satisfies the following scaling or refinement equation

$$\varphi(x) = 2^{d/2} \sum_{k \in \mathbb{Z}^d} h_k \varphi(2x - k). \tag{3.1}$$

In the sequel we will only be concerned with compactly supported scaling functions. The sequence of real numbers $\{h_k\}$ is finite then.

We further require the standardization $\int_{\mathbb{R}^d} \varphi(x) \, dx = 1$ and that the integer translates $\{\varphi(\cdot - k) \mid k \in \mathbb{Z}^d\}$ generate a Riesz system in $L^2(\mathbb{R}^d)$.

Next we define a family $\{V_l\}_{l \in \mathbb{Z}}$ of spaces closely related to φ by

$$V_l := \text{clos}_{L^2(\mathbb{R}^d)} (\text{span}\{\varphi_{l,k} \mid k \in \mathbb{Z}^d\})$$

where $f_{l,k}(\cdot) := 2^{-dl/2} f(2^l \cdot - k)$ for $f \in L^2(\mathbb{R}^d)$. Obviously, the spaces $\{V_l\}$ are nested due to (3.1), that is, $V_l \subset V_{l+1}$. See Chapter 5.3 in [18] for further properties of $\{V_l\}$.

Definition 3.1. We say a scaling function φ admits a set of *wavelets* $\{\psi_e \mid e \in E\} \subset L^2(\mathbb{R}^d)$, $E = \{0, 1\}^d \setminus \{0\}$, iff:

1. $V_{l+1} = V_l \oplus W_l$ with $W_l = \bigoplus_{e \in E} W_{e,l}$ where the sums are direct sums and where

$$W_{e,l} := \text{clos}_{L^2(\mathbb{R}^d)} (\text{span}\{\psi_{e,l,k} \mid k \in \mathbb{Z}^d\}).$$

2. The set $\{\psi_{e,j,k} \mid j \in \mathbb{Z}, k \in \mathbb{Z}^d, e \in E\}$ is a Riesz basis for $L^2(\mathbb{R}^d)$.

We call φ a *biorthogonal* scaling function if there is another compactly supported scaling function $\tilde{\varphi}$ (a *dual* to φ) with wavelets $\{\tilde{\psi}_e \mid e \in E\}$ such that $\langle \varphi_{0,k}, \tilde{\varphi}_{0,m} \rangle_{L^2} = \delta_{k,m}$ as well as

$$\langle \psi_{e,0,k}, \tilde{\psi}_{\epsilon,0,m} \rangle_{L^2} = \delta_{e,\epsilon} \delta_{k,m} \text{ and } \langle \varphi_{0,k}, \tilde{\psi}_{\epsilon,0,m} \rangle_{L^2} = \langle \tilde{\varphi}_{0,k}, \psi_{\epsilon,0,m} \rangle_{L^2} = 0. \tag{3.2}$$

We will only deal with scaling functions φ related to a biorthogonal wavelet system $\{\varphi, \tilde{\varphi}, \psi_e, \tilde{\psi}_e \mid e \in E\}$ where all functions involved have compact support.

Typical examples for biorthogonal scaling functions are B-splines (see [8]), the Daubechies scaling functions (see [17]), and tensor products thereof. Further, several kinds of (non-tensor-type) box splines belong to this category as well, see *e.g.* [10].

A scaling function φ is of *order* N if the polynomials up to degree $N-1$ can be expressed by linear combinations of integer translates of φ .

Order N biorthogonal scaling functions allow a characterization of the Sobolev spaces

$$H^s(\mathbb{R}^d) := \left\{ f \in L^2(\mathbb{R}^d) \mid \|f\|_{H^s(\mathbb{R}^d)}^2 := \int_{\mathbb{R}^d} (1 + \|\omega\|_{\mathbb{R}^d}^2)^s |\hat{f}(\omega)|^2 \, d\omega < \infty \right\} \tag{3.3}$$

by an equivalent discrete norm. In (3.3), \hat{f} denotes the Fourier transform of f . We have that, see Dahmen [11] or [12],

$$\|f\|_{H^s(\mathbb{R}^d)}^2 \asymp \sum_{k \in \mathbb{Z}^d} |\langle f, \tilde{\varphi}_{0,k} \rangle_{L^2}|^2 + \sum_{j=0}^{\infty} 2^{2sj} \sum_{k \in \mathbb{Z}^d} \sum_{e \in E} |\langle f, \tilde{\psi}_{e,j,k} \rangle_{L^2}|^2 \tag{3.4}$$

for $0 \leq s < \min\{N, s_{\max}\}$ where s_{\max} is the maximal Sobolev regularity of φ defined by

$$s_{\max} := \sup \{t \mid \varphi \in H^t(\mathbb{R}^d)\}. \tag{3.5}$$

Our notation $A \asymp B$ used in (3.4) is equivalent to $A \preceq B \preceq A$ where $A \preceq B$ indicates the existence of a generic constant $c > 0$ such that $A \leq cB$. The constant c will not depend on the arguments of A and B .

We now introduce a periodic setting due to Meyer [30]. Essential properties of biorthogonal scaling functions carry over to their periodized versions.

Let f be a compactly supported square integrable function. We define its periodization $[f] \in L^2(\mathcal{T}^d)$ by $[f](\cdot) := \sum_{r \in \mathbb{Z}^d} f(\cdot + r)$. For convenience we set

$$f_k^l := [f_{l,k}].$$

With a biorthogonal scaling function φ we associate the spaces V_l^p (3.6), $l \in \mathbb{N}_0$, of dimension 2^{dl} ,

$$V_l^p := \text{span} \{ \varphi_k^l \mid k \in \mathbb{Z}^{d,l} \} \subset L^2(\mathcal{T}^d), \tag{3.6}$$

where $\mathbb{Z}^{d,l} := \mathbb{Z}^d / (2^l \mathbb{Z}^d)$. The refinement equation (3.1) is inherited by φ_k^l . Consequently, the spaces V_l^p are nested, *i.e.*, $V_l^p \subset V_{l+1}^p$. Furthermore, we have the wavelet splitting

$$V_l^p = V_{l-1}^p \oplus \bigoplus_{e \in E} W_{e,l-1}^p \quad \text{where } W_{e,j}^p = \text{span} \{ \psi_{e,k}^j \mid k \in \mathbb{Z}^{d,j} \}. \tag{3.7}$$

The Sobolev spaces $H^s(\mathcal{T}^d)$ are characterized by a periodic version of the norm equivalence (3.4), see *e.g.* [12].

3.2. Galerkin scheme for (2.1)

We choose the spaces V_l^p (3.6) as approximation spaces in our Galerkin scheme. These spaces are subspaces of $H^1(\mathcal{T}^d)$ provided the underlying biorthogonal scaling function φ is in $H^1(\mathbb{R}^d)$ which we assume.

It will prove convenient to use the following notation. We define the index set

$$\mathcal{B}_l := \{ m \in \mathbb{Z}^{d,l} \mid \text{int}(\text{supp } \varphi_m^l \cap \square) \cap \partial\Omega \neq \emptyset \} \tag{3.8}$$

which contains the indices of basis functions whose supports intersect the boundary of Ω (\mathcal{B} for *boundary*). Next we introduce the approximation $\gamma^l : V_l^p \rightarrow V_l^p$ to the trace operator γ :

$$\gamma^l(v_l) := \sum_{k \in \mathcal{B}_l} v_{l,k} \varphi_k^l, \quad \text{if } v_l = \sum_{k \in \mathbb{Z}^{d,l}} v_{l,k} \varphi_k^l, \quad v_{l,k} \in \mathbb{R}.$$

Our last ingredient is the function

$$g_l := \sum_{k \in \mathcal{B}_l} \langle g, \tilde{\varphi}_k^l \rangle_{L^2(\mathcal{T}^d)} \varphi_k^l \in V_l^p \tag{3.9}$$

whose trace γg_l approximates the boundary value g , *cf.* (1.1b). In (3.9), $\tilde{\varphi}$ is a dual scaling function to φ and g denotes a smooth extension of the boundary data g (here again we rely on the existence of such an extension, compare Rem. 2.1).

Now we are ready to discretize (2.1) by the variational problem (3.10),

$$\begin{cases} \text{find } u_l \in V_l^p \text{ with } \gamma^l(u_l) = \gamma^l(g_l) \text{ such that} \\ a(u_l, v_l) = \langle f, v_l \rangle_{L^2(\mathcal{T}^d)} \quad \forall v_l \in V_l^p \text{ with } \gamma^l(v_l) = 0. \end{cases} \tag{3.10}$$

Under our hypotheses problem (3.10) has a unique solution u_l .

The error estimates for u_l proved in Chapter 4 of [33] are non-optimal for $u \in H^{1+t}(\Omega)$ with $t \geq 1/2$ (see (4.8) below). This happens because the boundary constraint in (3.10) limits the flexibility of u_l on the strip

$$\partial\Omega^l := \bigcup_{m \in \mathcal{B}_l} \text{supp } \varphi_{l,m}. \tag{3.11}$$

The width of $\partial\Omega^l$ is proportional to $\delta_l = 2^{-l}$ which denotes the *discretization step size* related to V_l^P . We therefore expect a higher accuracy of the numerical solution when resolving the boundary of Ω on a finer scale. The technical details will be elaborated in the next section.

4. A PRIORI ADAPTIVITY

The plan of attack is the following: we start with a full approximation space V_l^P where l is large enough to guarantee a small $H^1(\Omega)$ -error of u_l . Then we construct a subspace by coarsening V_l^P ‘away from the boundary of Ω ’.

4.1. Boundary resolution

Let φ be a biorthogonal scaling function and select an integer λ such that $0 \leq \lambda \leq l - 1$. According to (3.7) we have the multilevel splitting (4.1) of V_l^P :

$$V_l^P = V_\lambda^P \oplus \bigoplus_{j=\lambda}^{l-1} \bigoplus_{e \in E} W_{e,j}^P. \tag{4.1}$$

Denoting by $S_{j,k}^e$ and $\tilde{S}_{j,k}^e$ the smallest cubes in \mathbb{R}^d containing the supports of $\psi_{e,j,k}$ and $\tilde{\psi}_{e,j,k}$, respectively, we define the *sparse wavelet spaces* by

$$W_{e,j}^s := \text{span}\{\psi_{e,k}^j \mid k \in \mathcal{I}_j^e\}, \quad \lambda \leq j \leq l - 1,$$

where

$$\mathcal{I}_j^e = \mathcal{I}_j^{e,1} \cup \mathcal{I}_j^{e,2} \tag{4.2}$$

with

$$\mathcal{I}_j^{e,1} := \{m \in \mathbb{Z}^{d,j} \mid \text{int}(S_{j,m}^e) \cap \partial\Omega^l \neq \emptyset\}, \quad \mathcal{I}_j^{e,2} := \{m \in \mathbb{Z}^{d,j} \mid \text{int}(\tilde{S}_{j,m}^e) \cap \partial\Omega \neq \emptyset\}.$$

The sparse wavelet spaces essentially contain only those wavelets whose supports intersect the boundary strip $\partial\Omega^l$ (3.11). The *sparse approximation space*

$$V_{l,\lambda}^s := V_\lambda^P \oplus \bigoplus_{j=\lambda}^{l-1} \bigoplus_{e \in E} W_{e,j}^s \tag{4.3}$$

obviously resolves the boundary of Ω with a higher accuracy than the interior. Since $\mathcal{I}_j^{e,1} \subset \mathcal{I}_j^e$ we are able to realize the boundary constraint from (3.10) on $V_{l,\lambda}^s$. The additional index set $\mathcal{I}_j^{e,2}$ is included in the definition of \mathcal{I}_j^e for technical reasons which will become clear in Section 4.2 below. If the size of $\tilde{S}_{j,m}^e$ is not too large then $\mathcal{I}_j^e = \mathcal{I}_j^{e,1}$. Such a situation is considered in Figure 4.1 which gives an impression on a typical sparsity pattern of $V_{l,\lambda}^s$.

Next we estimate the degrees of freedom in $V_{l,\lambda}^s$. Since $\partial\Omega$ is $(d - 1)$ -dimensional compact manifold the cardinality of \mathcal{I}_j^e grows like $2^{(d-1)j}$ which yields

$$2^{d\lambda} \leq \dim V_{l,\lambda}^s \leq 2^{d\lambda} + 2^{(d-1)l}.$$

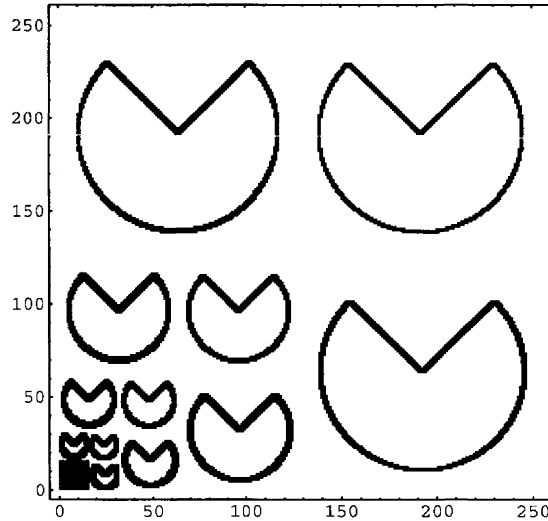


FIGURE 4.1. Sparsity pattern of $V_{8,4}^s$ with respect to the biorthogonal wavelet system used for the computational experiments in Section 5 below. The underlying domain $\Omega \subset \mathbb{R}^2$ is a circular disk with a re-entrant corner. Each basis function in $V_8^p = V_4^p \oplus \bigoplus_{j=4}^7 \bigoplus_{e \in E} W_{e,j}^p$ is uniquely represented by a pair (k_1, k_2) with $1 \leq k_i \leq 256$. The pixel (k_1, k_2) is colored black if the corresponding wavelet function belongs to $V_{8,4}^s$, otherwise, it remains uncolored. The dependence of \mathcal{I}_j^e on e can be observed. The 16×16 black square in the lower left corner shows that $V_4^p \subset V_{8,4}^s$. The full space V_8^p would be indicated by a black box of size 256×256 . Please note that $\dim V_{8,4}^s / \dim V_8^p \approx 0.11$.

The quantity on the right represents asymptotically the correct dimension of $V_{l,\lambda}^s$. Considering $\delta_\lambda = 2^{-\lambda}$ as the principal discretization step size related to $V_{l,\lambda}^s$ we obtain the optimal relation

$$\dim V_{l,\lambda}^s \asymp \delta_\lambda^{-d} \quad \text{iff} \quad l \leq d/(d-1)\lambda. \tag{4.4}$$

Now we discretize (2.1) by the variational problem (4.5) using sparse spaces,

$$\begin{cases} \text{find } u_{l,\lambda} \in V_{l,\lambda}^s \text{ with } \gamma^l(u_{l,\lambda}) = \gamma^l(g_l) \text{ such that} \\ a(u_{l,\lambda}, v_l) = \langle f, v_l \rangle_{L^2(\mathcal{T}^d)} \quad \forall v_l \in V_{l,\lambda}^s \text{ with } \gamma^l(v_l) = 0. \end{cases} \tag{4.5}$$

Of course, (4.5) has a unique solution $u_{l,\lambda}$. We bound its error in the following theorem.

Theorem 4.1. *Let φ be a biorthogonal scaling function of order $N \geq 2$ with $s_{\max} > 1$. Assume that u , the weak solution of (1.1), is in $H^{1+t}(\Omega)$ for a $0 < t \leq N - 1$. Then,*

$$\|u - u_{l,\lambda}\|_{H^1(\Omega)} \leq \|u - u_l\|_{H^1(\Omega)} + \delta_\lambda^t \|u\|_{H^{1+t}(\Omega)}. \tag{4.6}$$

If the homogeneous ($g = 0$) boundary value problem (1.1) is additionally H^2 -regular then

$$\|u - u_{l,\lambda}\|_{L^2(\Omega)} \leq \|u - u_l\|_{L^2(\Omega)} + (\delta_l^{1/2} + \delta_\lambda) \|u - u_{l,\lambda}\|_{H^1(\Omega)}. \tag{4.7}$$

Before we are going to prove the above theorem in Section 4.2 below let us discuss some of its implications. For simplicity we assume that $u \in H^N(\Omega)$. If g is sufficiently smooth in a neighborhood of Ω (g is an extension to

□ of the boundary value) then

$$\|u - u_l\|_{H^s(\Omega)} \preceq \delta_l^{1-s/2} \|u\|_{H^N(\Omega)}, \quad s = 0, 1 \tag{4.8}$$

(the proofs of Ths. 4.5 and 4.9 from [33] can be modified to yield the above estimate). Relating l and λ by $l = 2(N - 1) \cdot \lambda$ yields the optimal error bound (with respect to δ_λ)

$$\|u - u_{2(N-1)\cdot\lambda}\|_{H^s(\Omega)} \preceq \delta_\lambda^{N-s} \|u\|_{H^N(\Omega)}, \quad s = 0, 1. \tag{4.9}$$

We achieve this optimal error estimate under $\dim V_{2(N-1)\cdot\lambda}^s \approx \delta_\lambda^{-d} + \delta_\lambda^{-(d-1)2(N-1)}$. In view of (4.4) this number of degrees of freedom is optimal iff $d = 2$ and $N = 2$. This was to be expected due to results by Oswald (Chap. 5.2 in [31]).

An implementation of the above described adaptive scheme requires the knowledge of the index set \mathcal{I}_j^e (see (4.2)). Here one can rely on a technique introduced in Chap. 5.2 of [33] to classify the indices in \mathcal{B}_l (see (3.8)).

Remark 4.2. We will comment in some detail on the differences between our and Oswald’s boundary modifications. Especially, we argue that Oswald’s convergence result (Lem. 5 of [31]) does not imply our Theorem 4.1.

The sparse approximation spaces $\tilde{V}_{l,\lambda}^s$ of Oswald are spanned by scaling functions on different levels, that is,

$$\tilde{V}_{l,\lambda}^s = \text{span}\{\varphi_k^j \mid k \in \mathcal{O}_j, j = \lambda, \dots, l\}.$$

The index sets $\mathcal{O}_j \subset \mathbb{Z}^{d,j}$ are determined geometrically by a cube partition of Ω and contain – roughly speaking – the indices of level- j scaling functions which live “near” to the boundary of Ω . For $l > \lambda + 1$ there are geometric settings possible where we have φ_k^j ’s in $\tilde{V}_{l,\lambda}^s$ which are *not* in $V_{l,\lambda}^s$. The reason for this is simply that $V_{l,\lambda}^s$ does not contain enough wavelets to span all scaling functions on intermediate levels which intersect the boundary of Ω . Though both approaches are very similar in nature they are far from being equivalent.

4.2. Proof of Theorem 4.1

This section is completely occupied with the proof of Theorem 4.1. By a simple triangle inequality it suffices to estimate $\|u_l - u_{l,\lambda}\|_{H^s(\Omega)}$ for $s = 0, 1$.

First, we will verify that

$$\|u_l - u_{l,\lambda}\|_{H^1(\Omega)} \preceq \delta_\lambda^\kappa \|u - u_l\|_{H^{1+\kappa}(\Omega)} + \delta_\lambda^t \|u\|_{H^{1+t}(\Omega)} \tag{4.10}$$

where $0 \leq \kappa < \min\{s_{\max} - 1, t\}$. Clearly, (4.10) implies (4.6). Following the line of proof of Theorem 4.1 in [33] we obtain

$$\|u_l - u_{l,\lambda}\|_{H^1(\Omega)} \preceq \inf \{ \|u_l - w_l\|_{H^1(\Omega)} \mid w_l \in V_{l,\lambda}^s, \gamma^l(w_l) = \gamma^l(g_l) \} \tag{4.11}$$

which is a variation of Cea’s lemma, see *e.g.* p. 327 in [21]. Since $u_l \in V_l^p$ we have the expansion

$$u_l = \sum_{k \in \mathbb{Z}^{d,\lambda}} c_{\lambda,k} \varphi_k^\lambda + \sum_{j=\lambda}^{l-1} \sum_{e \in E} \sum_{m \in \mathbb{Z}^{d,j}} d_{e,j,m} \psi_{e,m}^j,$$

see (4.1), where $c_{\lambda,k} = \langle u_l, \tilde{\varphi}_k^\lambda \rangle_{L^2(\mathcal{T}^d)}$ and $d_{e,j,m} = \langle u_l, \tilde{\psi}_{e,m}^j \rangle_{L^2(\mathcal{T}^d)}$.

Using the above expansion coefficients of u_l we define

$$w_l := \sum_{k \in \mathbb{Z}^{d,\lambda}} c_{\lambda,k} \varphi_k^\lambda + \sum_{j=\lambda}^{l-1} \sum_{e \in E} \sum_{m \in \mathcal{I}_j^e} d_{e,j,m} \psi_{e,m}^j$$

which is in $V_{l,\lambda}^s$ satisfying $\gamma^l(w_l) = \gamma^l(u_l) = \gamma^l(g_l)$. Thus, (4.11) leads to

$$\|u_l - u_{l,\lambda}\|_{H^1(\Omega)} \preceq \left\| \sum_{j=\lambda}^{l-1} \sum_{e \in E} \sum_{m \in \mathbb{Z}^{d,j} \setminus \mathcal{I}_j^e} d_{e,j,m} \psi_{e,m}^j \right\|_{H^1(\Omega)}. \tag{4.12}$$

The definition of \mathcal{I}_j^e (see (4.2)) justifies to replace the periodized wavelets in the right-hand side of (4.12) by their original versions:

$$\|u_l - u_{l,\lambda}\|_{H^1(\Omega)} \preceq \left\| \sum_{j=\lambda}^{l-1} \sum_{e \in E} \sum_{m \in \mathcal{J}_j^e} d_{e,j,m} \psi_{e,j,m} \right\|_{H^1(\mathbb{R}^d)}$$

with the index set

$$\mathcal{J}_j^e := \{m \in \mathbb{Z}^d \mid \text{int}(S_{j,m}^e) \subset \Omega\} \cap \{m \in \mathbb{Z}^d \mid \text{int}(\tilde{S}_{j,m}^e) \subset \Omega\}.$$

In our calculations below we will frequently use that $\tilde{S}_{j,m}^e$ is a subset of Ω for $m \in \mathcal{J}_j^e$. To guarantee the latter inclusion we added $\mathcal{I}_j^{e,2}$ to the definition of \mathcal{I}_j^e , see (4.2).

The norm equivalence (3.4) yields

$$\|u_l - u_{l,\lambda}\|_{H^1(\Omega)}^2 \preceq \sum_{j=\lambda}^{l-1} \delta_j^{-2} \sum_{e \in E} \sum_{m \in \mathcal{J}_j^e} |d_{e,j,m}|^2. \tag{4.13}$$

For $m \in \mathcal{J}_j^e$ we have $d_{e,j,m} = \langle u_l - u, \tilde{\psi}_{e,j,m} \rangle_{L^2(\tilde{S}_{j,m}^e)} + \langle u, \tilde{\psi}_{e,j,m} \rangle_{L^2(\tilde{S}_{j,m}^e)}$ so that

$$|d_{e,j,m}|^2 \preceq |\langle u_l - u, \tilde{\psi}_{e,j,m} \rangle_{L^2(\tilde{S}_{j,m}^e)}|^2 + |\langle u, \tilde{\psi}_{e,j,m} \rangle_{L^2(\tilde{S}_{j,m}^e)}|^2. \tag{4.14}$$

As a direct consequence of (3.2) we state that

$$\int_{\mathbb{R}^d} x^\beta \tilde{\psi}_e(x) dx = 0 \text{ for all } \beta \in \mathbb{N}_0^d \text{ with } |\beta| \leq N - 1 \text{ and for all } e \in E.$$

Since the diameter of $\tilde{S}_{j,m}^e$ is proportional to δ_j , the vanishing moments of $\tilde{\psi}_e$ immediately imply the estimate

$$|\langle w, \tilde{\psi}_{e,j,m} \rangle_{L^2(\tilde{S}_{j,m}^e)}| \preceq \delta_j^s \|w\|_{H^s(\tilde{S}_{j,m}^e)}, \quad 0 \leq s \leq N, \tag{4.15}$$

whenever the right-hand side is finite (see Th. 2 in [3]).

Due to our assumptions on $\partial\Omega$ there exists a bounded linear extension operator $F_\Omega : H^{1+\kappa}(\Omega) \rightarrow H^{1+\kappa}(\mathbb{R}^d)$ with $F_\Omega f = f$ a.e. in Ω (see e.g. Chap. VI in [34]). Because u_l is in $H^{1+\kappa}(\Omega)$ we may estimate as follows

$$\begin{aligned} & \sum_{j=\lambda}^{l-1} \delta_j^{-2} \sum_{e \in E} \sum_{m \in \mathcal{J}_j^e} |\langle u_l - u, \tilde{\psi}_{e,j,m} \rangle_{L^2(\tilde{S}_{j,m}^e)}|^2 \\ & \leq \sum_{j=\lambda}^{l-1} \delta_j^{-2} \sum_{e \in E} \sum_{m \in \mathbb{Z}^d} |\langle F_\Omega(u_l - u), \tilde{\psi}_{e,j,m} \rangle_{L^2(\tilde{S}_{j,m}^e)}|^2 \\ (4.15) \quad & \preceq \sum_{j=\lambda}^{l-1} \delta_j^{2\kappa} \sum_{e \in E} \sum_{m \in \mathbb{Z}^d} \|F_\Omega(u - u_l)\|_{H^{1+\kappa}(\tilde{S}_{j,m}^e)}^2 \preceq \sum_{j=\lambda}^{l-1} \delta_j^{2\kappa} \|F_\Omega(u_l - u)\|_{H^{1+\kappa}(\mathbb{R}^d)}^2 \\ & \preceq \delta_\lambda^{2\kappa} \|F_\Omega(u_l - u)\|_{H^{1+\kappa}(\mathbb{R}^d)}^2 \preceq \delta_\lambda^{2\kappa} \|u_l - u\|_{H^{1+\kappa}(\Omega)}^2. \end{aligned}$$

By (4.13), (4.14), and the latter inequality we get

$$\|u_l - u_{l,\lambda}\|_{H^1(\Omega)}^2 \preceq \delta_\lambda^{2\kappa} \|u - u_l\|_{H^{1+\kappa}(\Omega)}^2 + \sum_{j=\lambda}^{l-1} \delta_j^{-2} \sum_{e \in E} \sum_{m \in \mathcal{J}_j^e} |\langle u, \tilde{\psi}_{e,j,m} \rangle_{L^2(\tilde{S}_{j,m}^e)}|^2.$$

It remains to estimate the rightmost term. From (4.15) we infer that

$$\begin{aligned} \sum_{j=\lambda}^{l-1} \delta_j^{-2} \sum_{e \in E} \sum_{m \in \mathcal{J}_j^e} |\langle u, \tilde{\psi}_{e,j,m} \rangle_{L^2(\tilde{S}_{j,m}^e)}|^2 & \preceq \sum_{j=\lambda}^{l-1} \delta_j^{2t} \sum_{e \in E} \sum_{m \in \mathcal{J}_j^e} \|u\|_{H^{1+t}(\tilde{S}_{j,m}^e)}^2 \\ & \preceq \sum_{j=\lambda}^{l-1} \delta_j^{2t} \|u\|_{H^{1+t}(\Omega)}^2 \preceq \delta_\lambda^{2t} \|u\|_{H^{1+t}(\Omega)}^2. \end{aligned}$$

Thus, we have established (4.10) and (4.6) thereupon.

Now we turn to the proof of (4.7). We consider the auxiliary homogeneous problem (4.16) with $e = u_l - u_{l,\lambda} \in H_0^1(\Omega)$:

$$\begin{cases} \text{find } w \in H_0^1(\Omega) \text{ such that} \\ b(w, v) = \langle e, v \rangle_{L^2(\Omega)} \quad \forall v \in H_0^1(\Omega). \end{cases} \tag{4.16}$$

In (4.16), b is adjoint to a , that is, $b(w, v) = a(v, w)$ (here a and b are restricted to Ω). Due to the assumed H^2 -regularity we have for the unique solution w of (4.16) that

$$\|w\|_{H^2(\Omega)} \preceq \|e\|_{L^2(\Omega)}. \tag{4.17}$$

By the duality argument of Aubin-Nitsche (see e.g. Chap. 3.2 in [6]) we get

$$\|e\|_{L^2(\Omega)}^2 \preceq \|e\|_{H^1(\Omega)} \inf \{ \|w - z_{l,\lambda}\|_{H^1(\Omega)} \mid z_{l,\lambda} \in V_{l,\lambda}^s \text{ with } \text{supp} z_{l,\lambda} \subset \Omega \}.$$

We have already bound the infimum (see the proof for (4.6)) so that

$$\|e\|_{L^2(\Omega)}^2 \preceq \|e\|_{H^1(\Omega)} (\|w - w_l\|_{H^1(\Omega)} + \delta_\lambda \|w\|_{H^2(\Omega)})$$

where $w_l \in V_l^p$ is the solution of (3.10) with a and f replaced by b and e , respectively, and with $g = g_l = 0$. By (4.8) and (4.17) we finally find

$$\|u_l - u_{l,\lambda}\|_{L^2(\Omega)} \leq (\delta_l^{1/2} + \delta_\lambda) \|u_l - u_{l,\lambda}\|_{H^1(\Omega)}$$

which finishes the proof of (4.7).

5. NUMERICAL EXPERIMENTS

We illustrate the error estimates proved in the previous section by computational results. The implementational details and further examples can be found in [32, 33].

We solve the 2D-elliptic problem ($\Delta = \sum_{i=1}^2 D^{2e_i}$ is the Laplace operator)

$$-0.01 \Delta u + u = 1 \quad \text{in } \Omega, \tag{5.1a}$$

$$u = 0 \quad \text{on } \partial\Omega, \tag{5.1b}$$

with respect to the disk

$$\Omega = \left\{ x \in \mathbb{R}^2 \mid x_1^2 + x_2^2 < 1/16 \right\}.$$

The box $\square =]-0.3, 0.3]^2$ serves as fictitious domain. This example is considered because we know its exact solution u given by

$$u(x_1, x_2) = 1 - \frac{J_0(\iota 10 \sqrt{x_1^2 + x_2^2})}{J_0(\iota 5/2)}, \quad \iota = \sqrt{-1},$$

where J_0 is the Bessel function of the first kind of order 0. We are thus able to compute the error $u - u_{l,\lambda}$ on Ω .

In Chapter 6.A of [8] Cohen *et al.* constructed univariate biorthogonal wavelet systems $\{b_N, N, \tilde{N} \tilde{\varphi}, N, \tilde{N} \tilde{\psi}, N, \tilde{N} \tilde{\psi}\}$, $N + \tilde{N}$ even, where b_N is the cardinal B-Spline of order N (except for b_N we adopted the notation of [8]). Tensor products of those four functions can be used to create a bivariate biorthogonal wavelet system of order N (see *e.g.* [18] or [29]). The corresponding scaling function is the tensor product B-Spline $B_N = b_N \otimes b_N$, that is,

$$B_N(x) = B_N(x_1, x_2) = b_N(x_1) b_N(x_2).$$

Our computations below will be based on the linear ($N = 2$) B-spline biorthogonal wavelet system. The maximal Sobolev order of B_N is $s_{\max} = N - 1/2$. As the periodization $(B_N)_k^l$ of $(B_N)_{l,k}$ is 1-periodic the re-scaling $(B_N)_k^l(x/0.6)$ gives ansatz functions periodic with respect to \square .

We wish to illustrate the estimate (4.9). We therefore need a computable approximation to $\|v\|_{H^s(D)}$ where $D \subset \mathbb{R}^2$ is a bounded domain. In view of (3.4) we define

$$\text{norm}_{l,s}(v)_D := \left(\sum_{k \in \mathbb{Z}^2} |c_{2,k}|^2 + \sum_{j=2}^{l-1} \delta_j^{-2s} \sum_{m \in \mathbb{Z}^2} \sum_{e=1}^3 |d_{e,j,m}|^2 \right)^{1/2}$$

with $c_{2,k} = \langle v, (\tilde{B}_2)_{2,k} \rangle_{L^2(D)}$ and $d_{e,j,m} = \langle v, \tilde{\psi}_{e,j,m} \rangle_{L^2(D)}$.

Above, $\tilde{B}_2 = {}_{2,2} \tilde{\varphi} \otimes {}_{2,2} \tilde{\varphi}$ is the dual to B_2 and $\tilde{\psi}_e, e = 1, 2, 3$, are the three corresponding dual wavelets. The coefficients $c_{2,k}$ and $d_{e,j,m}$ (only finitely many are non-zero) can easily be obtained from v by a fast wavelet decomposition, see *e.g.* [18, 29]. Hence, a numerical value for $\text{norm}_{l,s}(v)_D$ can be calculated.

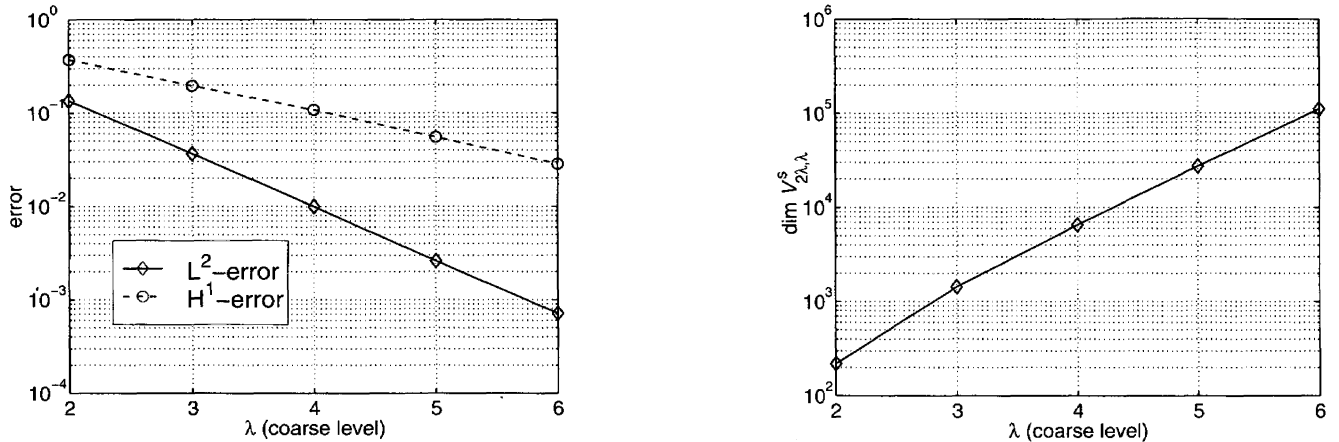


FIGURE 5.1. Left: $\text{norm}_{2\lambda,s}(u - u_{2\lambda,\lambda})_\Omega$ as function of λ for $s = 0$ (solid line with \diamond) and $s = 1$ (dashed line with \circ). Right: $\dim V_{2\lambda,\lambda}^s$.

Lemma 5.1. *Let v be in $H^r(\mathbb{R}^2)$ with $\text{supp } v \subset D$. Then, for $0 \leq s < 3/2$ and $s < r$, we have that*

$$\text{norm}_{l,s}(v)_D \preceq \|v\|_{H^s(D)} \preceq \text{norm}_{l,s}(v)_D + \delta_l^{\min\{2,r\}-s} \|v\|_{H^{\min\{2,r\}}(D)}.$$

Proof. The left inequality is an immediate consequence of the norm equivalence (3.4). The inequality on the right hand side results from a combination of (3.4) with (4.15). \square

Let $e_\lambda = u - u_{2\lambda,\lambda}$ be the error of the solution of (4.5) with $l = 2\lambda$ and with respect to the linear B-spline wavelet system (the technique for preconditioning problem (3.10) (see Chap. 6 in [33]) applies to (4.5) in particular). Since e_λ is in $H_0^1(\Omega) \cap H^r(\Omega)$ for any $r < 3/2$ we expect, in view of (4.9), that

$$\text{norm}_{2\lambda,s}(e_\lambda)_\Omega \preceq \delta_\lambda^{2-s}, \quad s = 0, 1.$$

Moreover, according to Lemma 5.1 the above decay rate of $\text{norm}_{2\lambda,s}(e_\lambda)_\Omega$ is sharp as $\lambda \rightarrow \infty$. Figure 5.1 displays $\text{norm}_{2\lambda,s}(e_\lambda)_\Omega$ for $s = 0, 1$ as a function of λ on a logarithmic scale. The predicted decay is clearly visible. On the right of Figure 5.1 we plotted $\dim V_{2\lambda,\lambda}^s$ to illustrate (4.4). The dimension of $V_{2\lambda,\lambda}^s$ increases by factor 4 with λ .

Figure 5.2 gives a graphic impression of (4.6) and (4.7) for fixed $\lambda = 2$. As l grows we first observe the decay rates (4.8) and then a saturation of the error due to fixed λ .

6. CONCLUDING REMARKS

The stiffness matrix relative to (4.5) is not sparse in general. It possesses the typical ‘‘finger structure’’ as there is a coupling of wavelets to different resolution levels.

Two ways are known in the literature to overcome this drawback. First, one may apply matrix or operator compression techniques as investigated, *e.g.*, by Dahmen *et al.* [14]. Second, the so-called non-standard (NS) operator representation in a wavelet basis (see [2]) leads to a decoupling of different resolution levels. Consequently, the corresponding stiffness matrix has a kind of band structure. In case of a constant coefficient differential operator only 2^d coefficient vectors have to be stored (their dimensions and hence the band width depend on the scaling function). From those the matrix entries can be retrieved by simple scaling. Moreover, the NS approach can even be enhanced by matrix compression (see [2, 14]). The price to pay is a doubling of the dimension compared to the standard representation.

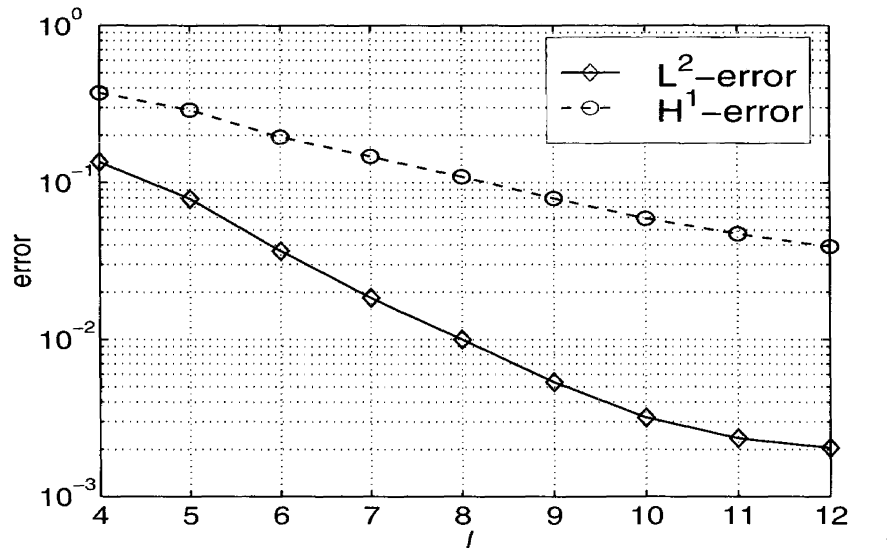


FIGURE 5.2. $\text{norm}_{l,s}(u - u_{l,2})_{\Omega}$ as function of l for $s = 0$ (solid line with \diamond) and $s = 1$ (dashed line with \circ).

The boundary treatment proposed here (and before in [27, 31]) for wavelet-based discretizations is not sophisticated enough to compete with traditional finite element discretizations. (With one exception: $d = 2$ and linear splines where the handling of complicated boundaries is even simpler.) To take full advantage of the wavelet machinery smarter techniques are required. Ideally these techniques provide accurate boundary resolution *without* depending too much on the geometry of the domain to retain (more or less) the issues (i)-(ii) from Section 1. Right now we do not know whether we will accomplish our goal, however, the potential gain justifies a further exploration of the proposed scheme.

REFERENCES

- [1] A. Barinka, T. Barsch, P. Charton, A. Cohen, S. Dahlke, W. Dahmen and K. Urban, Adaptive wavelet schemes for elliptic problems: implementation and numerical experiments. Tech. Report 173, Institut für Geometrie und Praktische Mathematik, RWTH Aachen, 52056 Aachen, Germany (1999).
- [2] G. Beylkin, R. Coifman and V. Rokhlin, Fast wavelet transforms and numerical algorithms I. *Comm. Pure Appl. Math.* **44** (1991) 141–183.
- [3] J.H. Bramble and S.R. Hilbert, Estimation of linear functionals on Sobolev spaces with application to Fourier transforms and spline interpolation. *SIAM J. Numer. Anal.* **7** (1970) 112–124.
- [4] W. Cai and W. Zhang, An adaptive spline wavelet ADI(SW-ADI) method for two-dimensional reaction diffusion equations. *J. Comput. Phys.* **139** (1998) 92–126.
- [5] C. Canuto, A. Tabacco and K. Urban, The wavelet element method, part I: construction and analysis. *Appl. Comput. Harmon. Anal.* **6** (1999) 1–52.
- [6] P.G. Ciarlet, The Finite Element Method for Elliptic Problems. *Stud. Math. Appl.* **4**, North-Holland, Amsterdam (1978).
- [7] A. Cohen, W. Dahmen and R. DeVore, Adaptive wavelet methods for elliptic operator equations – convergence rates. *Math. Comp.* posted on May 23, 2000, PII S0025-5718(00)01252-7 (to appear in print).
- [8] A. Cohen, I. Daubechies and J.-C. Feauveau, Biorthogonal bases of compactly supported wavelets. *Comm. Pure Appl. Math.* **45** (1992) 485–560.
- [9] S. Dahlke, W. Dahmen, R. Hochmuth and R. Schneider, Stable multiscale bases and local error estimation for elliptic problems. *Appl. Numer. Math.* **23** (1997) 21–48.
- [10] S. Dahlke, V. Latour and K. Gröchenig, Biorthogonal box spline wavelet bases, in *Surface Fitting and Multiresolution Methods*, A.L. Méhauté, C. Rabut and L.L. Schumaker Eds., Vanderbilt University Press (1997) 83–92.
- [11] W. Dahmen, Stability of multiscale transformations. *J. Fourier Anal. Appl.* **2** (1996) 341–362.
- [12] W. Dahmen, Wavelet and multiscale methods for operator equations. *Acta Numer.* **6** (1997) 55–228.

- [13] W. Dahmen, A. Kurdila and P. Oswald Eds., Multiscale Wavelet Methods for Partial Differential Equations. *Wavelet Anal. Appl.* **6**, Academic Press, San Diego (1997).
- [14] W. Dahmen, S. Prössdorf and R. Schneider, Wavelet approximation methods for pseudodifferential equations. II. Matrix compression and fast solution. *Adv. Comput. Math.* **1** (1993) 259–335.
- [15] W. Dahmen and R. Schneider, Composite wavelet bases for operator equations. *Math. Comp.* **68** (1999) 1533–1567.
- [16] W. Dahmen and R. Stevenson, Element-by-element construction of wavelets satisfying stability and moment conditions. *SIAM J. Numer. Anal.* **37** (1999) 319–352.
- [17] I. Daubechies, Orthonormal bases of compactly supported wavelets. *Comm. Pure Appl. Math.* **41** (1988) 906–966.
- [18] I. Daubechies, Ten Lectures on Wavelets. *CBMS-NSF Ser. in Appl. Math.* **61**, SIAM Publications, Philadelphia (1992).
- [19] J. Fröhlich and K. Schneider, An adaptive wavelet-Galerkin algorithm for one- and two-dimensional flame computations. *Eur. J. Mech. B Fluids* **11** (1994) 439–471.
- [20] J. Fröhlich and K. Schneider, An adaptive wavelet-vaguelette algorithm for the solution of nonlinear PDEs. *J. Comput. Phys.* **130** (1997) 174–190.
- [21] R. Glowinski, Numerical Methods for Nonlinear Variational Problems. *Springer Ser. Comput. Phys.*, Springer-Verlag, New York (1984).
- [22] R. Glowinski, Finite element methods for the numerical simulation of incompressible viscous flow: Introduction to the control of the Navier-Stokes equations, in Vortex Dynamics and Vortex Methods, C.R. Anderson and C. Greengard Eds., *Lectures in Appl. Math.* **28**, Providence, AMS (1991) 219–301.
- [23] R. Glowinski, T.-W. Pan and J. Périaux, A fictitious domain method for Dirichlet problem and applications. *Comput. Methods Appl. Mech. Engrg.* **111** (1994) 283–303.
- [24] R. Glowinski, T.-W. Pan and J. Périaux, A Lagrange multiplier/fictitious domain method for the Dirichlet problem – generalizations to some flow problems. *Japan J. Indust. Appl. Math.* **12** (1995) 87–108.
- [25] R. Glowinski, T.-W. Pan and J. Périaux, Fictitious domain methods for the simulation of Stokes flow past a moving disk, in *Computational Fluid Dynamics '96*, J.A. Desideri, C. Hirsh, P. LeTallec, M. Pandolfi and J. Périaux Eds., Chichester, Wiley (1996) 64–70.
- [26] W. Hackbusch, Elliptic Differential Equations: Theory and Numerical Treatment. *Springer Ser. Comput. Math.* **18**, Springer-Verlag, Heidelberg (1992).
- [27] S. Jaffard, Wavelet methods for fast resolution of elliptic problems. *SIAM J. Numer. Anal.* **29** (1992) 965–986.
- [28] S. Jaffard and Y. Meyer, Bases d'ondelettes dans des ouverts de \mathbb{R}^n . *J. Math. Pures Appl.* **68** (1992) 95–108.
- [29] A.K. Louis, P. Maass and A. Rieder, Wavelets: Theory and Applications. *Pure Appl. Math.*, Wiley, Chichester (1997).
- [30] Y. Meyer, *Ondelettes et Opérateurs I: Ondelettes*. Actualités Mathématiques, Hermann, Paris (1990). English version: *Wavelets and Operators*, Cambridge University Press (1992).
- [31] P. Oswald, Multilevel solvers for elliptic problems on domains, in Dahmen *et al.* [13] 3–58.
- [32] A. Rieder, On embedding techniques for 2nd-order elliptic problems, in *Computational Science for the 21st Century*, M.-O. Bristeau, G. Etgen, W. Fitzgibbon, J.L. Lions, J. Périaux and M.F. Wheeler Eds., Wiley, Chichester (1997) 179–188.
- [33] A. Rieder, A domain embedding method for Dirichlet problems in arbitrary space dimension. *RAIRO Modél. Math. Anal. Numér.* **32** (1998) 405–431.
- [34] E.M. Stein, Singular Integrals and Differentiability Properties of Functions. *Princeton Math. Ser.* **22**, Princeton University Press, Princeton (1970).
- [35] J. Wloka, *Partial Differential Equations*. Cambridge University Press, Cambridge, UK (1987).